SSCL-381

Superconducting Super Collider Laboratory

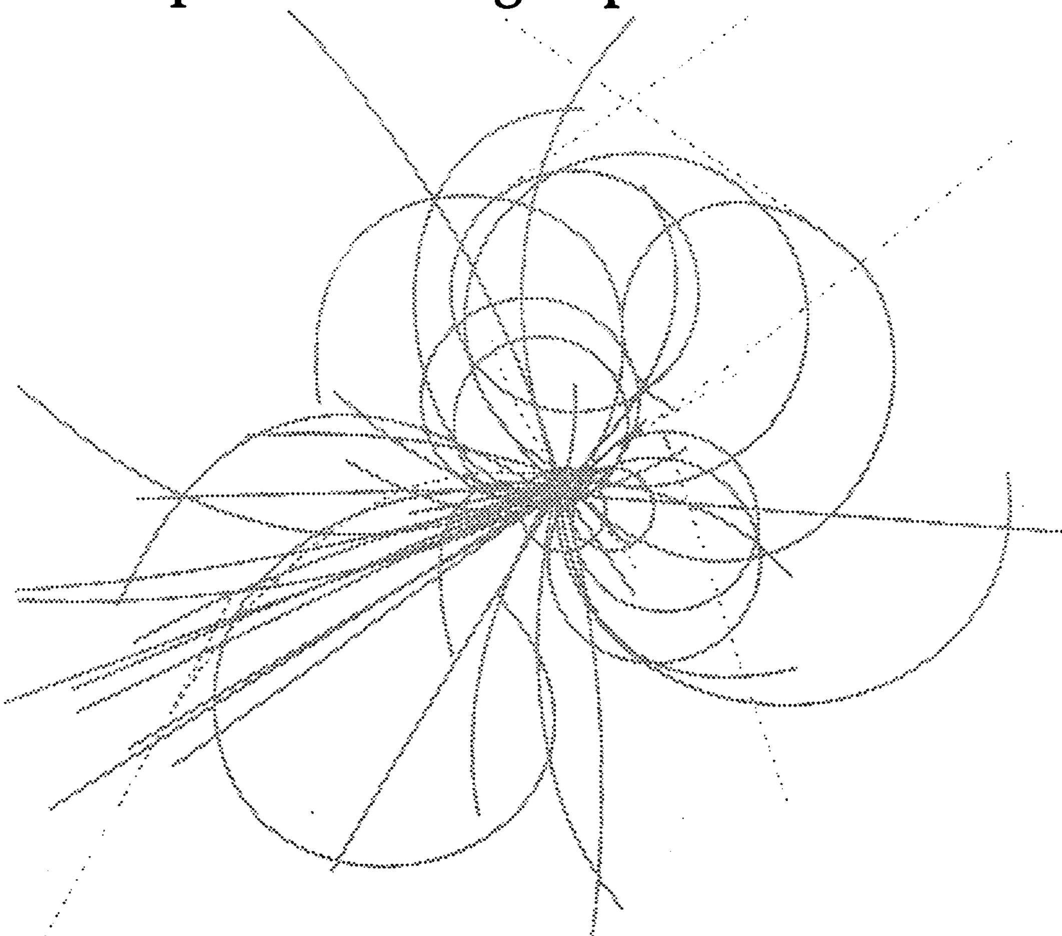

A Helium Venting Model for A SSC Half Cell

R. H. Carcagno, M. S. McAshan, and W. E. Schiesser

March 1991

To be published in Supercollider 3, Plenum Press, New York SSCL-381

A Helium Venting Model for A SSC Half Cell*

R. H. Carcagno, M. S. McAshan, and W. E. Schiesser

Accelerator Division
Superconducting Super Collider Laboratory†
2550 Beckleymeade Ave.
Dallas, TX 75237

March 1991

---

*Presented at the 1991 International Industrial Symposium on the Super Collider, Atlanta, Georgia, March 13–15, 1991.

†Operated by the Universities Research Association, Inc., for the U.S. Department of Energy under Contract No. DE-AC02-89ER40486.

A HELIUM VENTING MODEL FOR A SSC HALF CELL

R. H. Carcagno, M. S. McAshan, and W. E. Schiesser

Accelerator Division
Superconducting Super Collider Laboratory*
2550 Beckleymeade Avenue
Dallas, Texas 75237

Abstract: When a Superconducting Super Collider (SSC) dipole magnet quenches, the quench protection system will intentionally quench other magnets in the half cell. The result is that the stored energy of all of these quenched magnets will be absorbed equally among them. These simultaneous quenches produce heat, which diffuses from the magnet coils to the main helium (He) coolant channels and thereby eventually causes an increase in the He pressure. When the quench is detected, vent valves open to minimize the He pressure increase and thus prevent damage to the magnets.

The performance of the He venting system has been modeled and simulated to establish whether the venting will take place as required. The model consists of partial differential equation energy balances written radially for the magnet coils, collar, and yoke; and ordinary differential equations of energy and mass balance written for the He in the magnets and relief header. The basic algorithm is the numerical method of lines, with finite difference approximation of the spatial derivatives, and time integration by LSODES.

Simulation results will be presented for an SSC half cell of the Accelerator Systems String Test (ASST) facility. The results will be also compared with recent string quench measurements performed at the Fermilab String Test Facility.

*Operated by the Universities Research Association, Inc., for the U.S. Department of Energy under Contract No. DE-AC02-89ER40486.

INTRODUCTION

If a superconductor is warmed sufficiently, current no longer flows through it without resistance. The phenomenon of going from the superconductive state to the normal resistive state is called quenching. The electrical aspects of a quench and of quench protection systems are described elsewhere.[1,2] From the cryogenics point of view, an SSC magnet quench can be divided into the following three stages:

Stage One

While current is still flowing in a quenching magnet, Joule heating warms the He within and around the coils. As the temperature of the coils rises, trapped He in the cable expands and is expelled into the annular passage between the coils and the beam pipe (Figure 1). The He in this passage also receives heat from the coils by convective heat transfer. As a result of this mass and energy transfer, the He in the annular passage is expelled very rapidly into passages within the magnet cold mass and into the magnet interconnect region. The time constant of the first stage is less than a second because of the rapid current decay time constant in the coil. Assuming that the quench protection system works properly, the heat deposited in the coil is equal to the initial stored magnetic energy in the magnet. The energy stored in an SSC dipole at 6.6 T is 1.6 MJ. If this amount of heat is deposited evenly in the coil, the temperature increases to 70°K. However, the heat distribution in the coils immediately after the field decay is not uniform and is a complication in modeling the quench process during this stage.

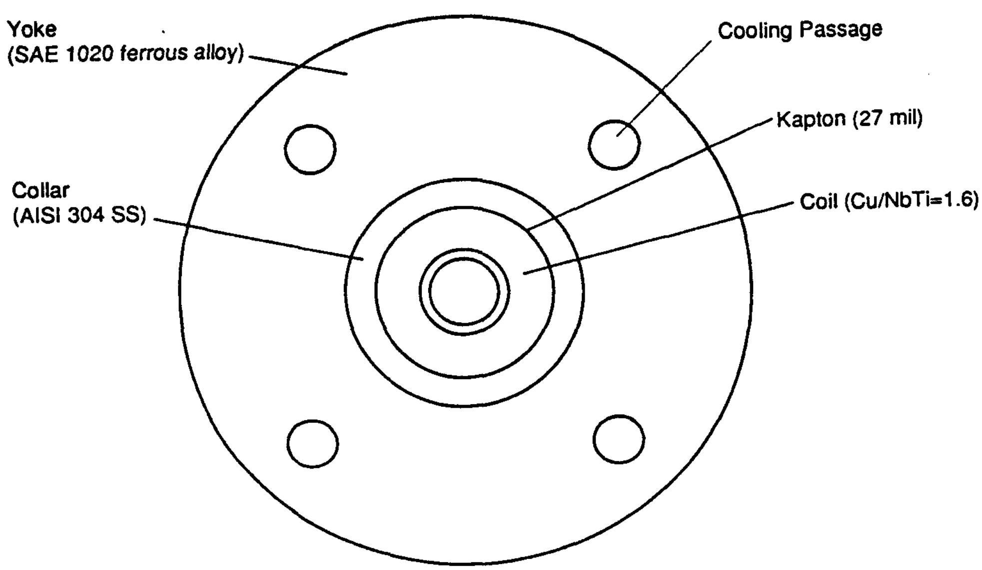

Figure 1. SSC Dipole Cold Mass Model for Heat Conduction.

Stage Two

During the second stage, most of the He will be vented from the half cell as the heat from the quench diffuses outward from the coils. This venting occurs through valves located in the spool pieces at each end of the quenching string (Figure 2). These valves open on signal from the quench detection electronics and automatically on pressure rise to vent into the 20K shield line. The pressure rise and venting rate on quench is determined in large part by the rate of diffusion of heat from the coils into the bulk of the He that is in the coolant channels in the iron. The heat must be conducted through the coil insulation, the stainless steel collars, and the iron itself, and the time constant of this process is on the order of several seconds. It is essential to provide an adequate venting system during this stage. For example, if no venting path is provided, the pressure will rise beyond 10 MPa as a result of the transfer of quench energy into the He at constant density. The time constant of the second stage is of the order of several seconds.

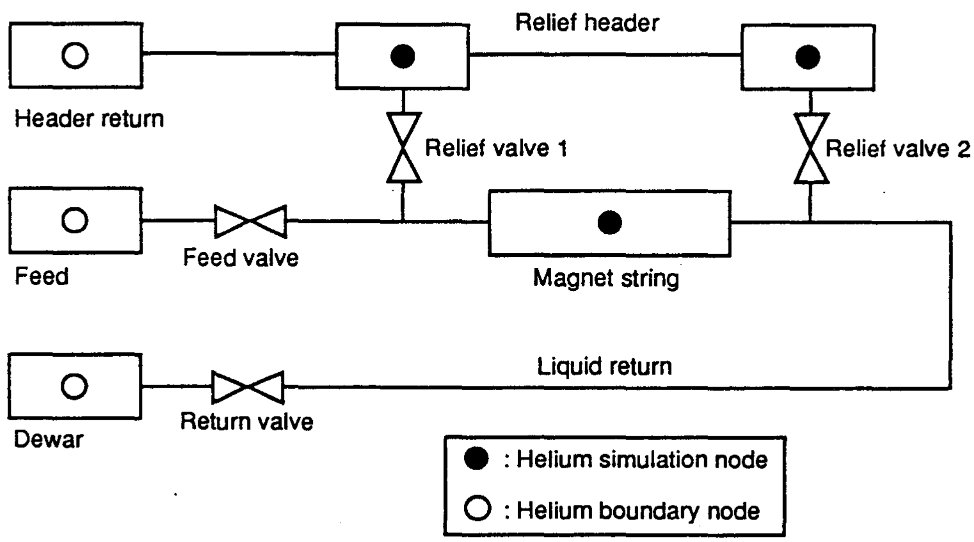

Figure 2. He Network for the SSC String Quench Venting Simulation Model.

Stage Three

In the third stage, which has a time constant of several minutes, all the He inventory has been vented, and the magnet is being cooled to the normal operating temperature.

In this paper we are mostly interested in a quench model for stage two. The pressure rise in stage one is too fast to be relieved by opening relief valves, and the pressure and temperature characteristics of stage three depend strongly on how the quench recovery strategy is implemented.

The performance of the venting system will affect primarily the pressure rise during the second stage. It is essential to understand the venting process and the time constant associated with it in order to design an appropriate venting system for the SSC. In this paper we present a model to simulate the SSC He venting system. This model was used to simulate the quench of a SSC half cell in the ASST.

The investigation of quench behavior is one of the primary goals of the half-cell test at Fermilab. The first quench measurements of a string of two magnets became available in early 1991. These measurements, together with modeling, are providing a quantitative basis for understanding the various aspects of the quench processes. We also present comparisons of simulation and measurements for a string quench in the Fermilab String Test facility.

MODEL DESCRIPTION

The venting model presented here includes an approximate model for the first quench stage and a detailed model for the second quench stage. The third quench stage relates to quench recovery, and its analysis is beyond the scope of this work. However, we are including the venting model in the process simulator SSCDYSIM[3] to study quench recovery in an SSC sector of 4 km of magnets.

Model for the First Stage

A simplified model is used to approximate the overall He pressure rise after the first quench stage. We assume that all the He mass trapped in the cable and in the annular passage is expelled into the bulk of the He in the main coolant channels and interconnect regions. The resulting temperature and pressure is calculated by assuming adiabatic compression of this volume.

For a more detailed treatment of this stage, see References 4 and 5.

Model for the Second Stage

The model for the second stage consists of the following three models:

(1) A model for heat conduction in the cold mass;

(2) A model for heat transfer to the bulk of the He that is in the main coolant channels in the iron; and

(3) A model for He venting through relief valves into a relief header.

Each of these models is discussed below.

Heat Conduction in the Cold Mass

Heat transfer in the cold mass is by conduction. The basic equation is then Fourier's second law for variable thermal properties, which in cylindrical coordinates is

$$\rho C_p \frac{\partial T}{\partial t} = \frac{1}{r}\frac{\partial}{\partial r}\left(rk\frac{\partial T}{\partial r}\right) + \frac{1}{r^2}\frac{\partial}{\partial \theta}\left(k\frac{\partial T}{\partial \theta}\right) + \frac{\partial}{\partial z}\left(k\frac{\partial T}{\partial z}\right). \tag{1}$$

If angular and axial variations in temperature are neglected, Equation (1) reduces to

$$\rho C_p \frac{\partial T}{\partial t} = \frac{1}{r}\frac{\partial}{\partial r}\left(rk\frac{\partial T}{\partial r}\right). \tag{2}$$

Equation (2) is the basic heat conduction equation for the cold mass; it is applied to the coils, with temperature $T_1(r,t)$, to the collar with temperature $T_2(r,t)$, and the yoke with temperature $T_3(r,t)$. Thus, we have the system of three PDEs:

$$\rho_1 C_{p1} \frac{\partial T_1}{\partial t} = \frac{1}{r}\frac{\partial}{\partial r}\left(rk_1\frac{\partial T_1}{\partial r}\right) \tag{3}$$

$$\rho_2 C_{p2} \frac{\partial T_2}{\partial t} = \frac{1}{r}\frac{\partial}{\partial r}\left(r k_2 \frac{\partial T_2}{\partial r}\right) \tag{4}$$

$$\rho_3 C_{p3} \frac{\partial T_3}{\partial t} = \frac{1}{r}\frac{\partial}{\partial r}\left(r k_3 \frac{\partial T_3}{\partial r}\right) + \frac{Q(r,t)}{V} . \tag{5}$$

Note that Equation (5) contains the term Q(r,t), which reflects the heat transfer with the He flowing through the main coolant channels. Variations of temperature with θ and z are neglected because (1) the axial conduction along the magnet is small (the collar and yoke are made of laminations), (2) calculation of the angular heat conduction indicates that it is also small compared to the radial conduction, and (3) the reduction of the model from three dimensions to one significantly reduces the complexity of the model and the associated computation of a solution. Variations of the physical properties have been included in the computer implementation of Equations (3), (4) and (5), i.e., $\rho = \rho(T)$, $C_p = C_p(T)$ and $k = k(T)$.

Equations (3), (4) and (5) each require one initial condition and two boundary conditions. Considering the boundary conditions first, we assume a zero gradient (no heat conduction) condition at the inner surface of the coils ($r = r_0$) and outer surface of the yoke ($r = r_3$)

$$k_1 \frac{\partial T_1(r_0,t)}{\partial r} = 0 \tag{6}$$

$$k_3 \frac{\partial T_3(r_3,t)}{\partial r} = 0 \ . \tag{7}$$

At the interface between the coils and the collar ($r = r_1$), and between the collar and the yoke ($r = r_2$), we assume that the rate of heat transfer is expressed in terms of contact resistances (C_{12}, C_{23}), i.e., there is a finite jump in temperature at these two interfaces:

$$k_1 \frac{\partial T_1(r_1,t)}{\partial r} = C_{12} \left(T_2 (r_1,t) - T_1(r_1,t)\right) \tag{8}$$

$$k_2 \frac{\partial T_2(r_1,t)}{\partial r} = C_{12} \left(T_2 (r_1,t) - T_1(r_1,t)\right) \tag{9}$$

$$k_2 \frac{\partial T_2(r_2,t)}{\partial r} = C_{23} \left(T_3 (r_2,t) - T_2(r_2,t)\right) \tag{10}$$

$$k_3 \frac{\partial T_2(r_2,t)}{\partial r} = C_{23} \left(T_3 (r_2,t) - T_2(r_2,t)\right). \tag{11}$$

Equations (6) to (11) are the required six boundary conditions.

For initial conditions, we use

$$T_1(r,0) = T_{10},\ T_2(r,0) = T_{20},\ T_3(r,0) = T_{30} \qquad (12),(13),(14)$$

where T_{10}, T_{20}, and T_{30} are prescribed initial conditions. Equations (3) to (14) are then the complete cold mass model (along with temperature-dependent properties).

Since this model is highly nonlinear (because of the strong dependence of the cold mass properties on temperature), we must use a numerical procedure for the solution of the model equations. We use a finite difference approximation of the right hand sides (RHS) of Equations (3) to (5), defined on a radial grid with index i. The finite difference approximation of the RHS conduction group at the interior grid points is then

$$\frac{1}{r}\frac{\partial}{\partial r}\left(rk\frac{\partial T}{\partial r}\right) \approx \frac{1}{r_i}\left(\frac{\left(\frac{r_{i+1}+r_i}{2}\right)\left(\frac{k(T_{i+1})+k(T_i)}{2}\right)\left(\frac{T_{i+1}-T_i}{\Delta r}\right) - \left(\frac{r_i+r_{i-1}}{2}\right)\left(\frac{k(T_i)+k(T_{i-1})}{2}\right)\left(\frac{T_i-T_{i-1}}{\Delta r}\right)}{\Delta r}\right) \qquad (15)$$

Boundary conditions (6) and (7) are approximated as

$$T_1(r_0 - \Delta r) = T_1(r_0 + \Delta r) \qquad (16)$$

$$T_3(r_3 - \Delta r) = T_3(r_3 + \Delta r) \qquad (17)$$

which are then substituted in Equation (15) as required, e.g., for the inner surface of the coils, i=1 in Equation (15) and T_{i-1} (= T_1 (r_0 - Δr)) is therefore a fictitious point which can be eliminated by substitution of Equation (16).

Boundary conditions (8) to (11) are substituted directly into Equation (15) with the grid index i set at values corresponding to the coils-collar ($r = r_1$) and collar-yoke ($r = r_2$) interfaces. Consequently, the three time derivatives in Equations (3), (4) and (5) can be computed at all of the radial grid points, including the boundaries and interfaces. This leads to a system of ordinary differential equations (ODEs), one ODE for each radial grid point; Equations (12), (13) and (14) are the required initial conditions. This system of ODEs is then added to the ODEs for the He to make up the complete magnet model.

We used the following materials in our cold mass model: for the yoke, SAE 1020 ferrous alloy; for the collar, AISI 304 Stainless Steel; and for the coils with a copper to superconductor (NbTi) ratio of 1.6. The contact thermal resistance between the coils and the collar (C_{12}) is equivalent to the conductivity of kapton divided by the kapton thickness between the coils and the collar (27 mil). Each region (coils, collar, and yoke) was discretized with seven radial grid points.

Heat Transfer to He

The term Q(r,t) in Equation (5) was calculated as

$$Q(r,t) = -hA\,(T_{wall} - T_{He}) \qquad (18)$$

In Equation (18), h is the heat transfer coefficient for rough walls. The main coolant channel is a pipe of rough walls because it is made out of iron laminations. The heat transfer coefficient h of a rough pipe can be obtained from the following expression :[6]

$$\frac{h}{h_{smooth}} = \sqrt{\frac{f}{f_{smooth}}}. \tag{19}$$

Equation (19) is valid for Pr ~ 1. The heat transfer coefficient for smooth pipes Re > 10000) can be obtained from Reference 7:

$$h_{smooth} = 0.023\ C_p\ G\ Re^{-0.2} Pr^{-2/3}. \tag{20}$$

A general expression for the Fanning friction factor is:[8]

$$\frac{1}{\sqrt{4f}} = -2 \log\left(\frac{\varepsilon/d}{3.7} + \frac{2.51}{Re\sqrt{4f}}\right) . \tag{21}$$

For smooth pipes, $\varepsilon = 0$. We used Equation (21) to calculate the ratio f/fsmooth, and then we used Equations (20) and (19) to calculate h.

He Venting Model

A basic assumption is that the lumped-parameter approach is adequate. A lump or node represents the capacitance or volume of an individual process vessel or group of vessels plus interconnecting piping. Within a lump or node, spatial variations of density, pressure, and temperature are assumed to be negligible. Therefore, homogeneous lumps can be modeled with first-order nonlinear ordinary differential equations. The lumped-parameter approach is commonly used for process simulation studies, and it appears to be adequate for the SSC quench simulation presented here; i.e., we do not expect spatial variation of the state variables to be significant.

The specific lumping assumptions made are illustrated in Figure 2. The magnet string was considered one node, and the relief header was split into two simulation nodes, one at each relief location.

Mass and energy balances were written for all nodes. The mass balance is

$$\frac{d\rho}{dt} = \frac{\left[\sum_{I=1}^{N} W_I - \sum_{J=N+1}^{M} W_J\right]}{V} . \tag{22}$$

with N input streams amd M output streams.

Assuming that no work is done on the surroundings and that there are negligible changes in kinetic and potential energies, the energy balance is

$$\frac{dU}{dt} = \frac{\left[\sum_{I=1}^{N} W_I(H_I - U) - \sum_{J=N+1}^{M} W_J(H_J - U) + Q\right]}{\rho V} . \tag{23}$$

Flow between nodes was assumed to be proportional to the square root of the product of the pressure difference and the density of the upstream node:

$$W = C\sqrt{\rho \Delta p} \quad . \tag{24}$$

The conductance C of the venting line is the only free parameter in our quench venting model. The value of this conductance was adjusted for agreement with the measured pressure level during venting for the Fermilab string quench.

For He properties, we used the international standard for the thermodynamic properties of He, the model developed by R. D. McCarty of NIST (formerly NBS) [9]

ASST HALF CELL QUENCH SIMULATION

A SSC half cell consists of a spool piece, five dipoles, one quadrupole, and seven interconnects. The total stored energy is about 8 MJ at 6.6 T. The He inventory in the half cell is about 0.6 m^3. We assume that 5% of the cable volume is filled with He, and that the beam pipe o.d. is 37 mm.

We assume that the stored energy is deposited evenly in the coils, raising the coil temperature to 70°K. The relief valves open immediately following a quench, venting He into the 20°K relief header. During venting, the temperature and pressure of the relief header change, affecting the peak pressure in the magnet during the process.

A description of the ASST quench model is given in Table 1.

Table 1. Boundary Conditions, Initial Conditions, and Parameters for the ASST Quench Model.

BOUNDARY CONDITIONS	PARAMETERS
Feed T = 4.5 K	Coil Inner Radius = 0.025 m
Feed P = 0.4 MPa	Coil Outer Radius = 0.050 m
Dewar T = 4.5 K	Kapton Thickness between coil and collar =
Dewar P = 0.12 MPa	6.85×10^{-4} m (27 mil)
Header Return T = 20 K	Collar Outer Radius = 0.068 m
Header Return P = 0.25 MPa	Yoke Outer Radius = 0.170 m
	Coolant Channel Diameter = 0.03175 m
	String Volume = 0.6 m^3
INITIAL CONDITIONS	He Mass in coils and in annular passage =
Coil T = 70 K	2.1 Kg/dipole
Collar, Yoke, and He T = 4.5 K	Relief Header Node Volume = 0.24 m^3
String P = 0.4 MPa	Relief Header Conductance = 0.00162 m^2
String Flow = 0.1 Kg/s	Relief Valve Conductance = 0.00068 m^2

Simulation Results

Figure 3 shows the string pressure as a function of time for two scenarios: venting through both relief valves and venting through relief valve 1 only. The first peak of about 1.5 MPa occurs as a consequence of adiabatic compression of the bulk of the He as the He mass in the coils and annular passage is expelled. As expected, this peak is the same for both scenarios. After the relief valves open, there is a rapid decrease in pressure. Eventually, the quench heat reaches the bulk of the He (Figure 4), and the pressure rises again to a second peak that depends on the number of relief valves open and is higher for the case of only one relief valve open. The second peak occurs during the stage two mentioned in the introduction. Most of the inventory venting will occur durng the second peak, as shown by Figure 5. The peak power input to the He is about 17 KW at 18 seconds, with a venting flow rate of about 2

Kg/s. Ninety percent of the inventory is vented in about 30 seconds, carrying away 23% of the quench energy.

Figure 6 shows the model mid-temperature of the coils, collar, yoke, and He as a function of time. The cold mass reaches an equilibrium temperature of 29°K at about 200 seconds.

Figure 7 shows the 20°K header pressure at the relief valve locations. Immediately after opening the relief valves the pressure decreases to almost 0.1 MPa because of the mixing of cold He with warm He. Later, the pressure rises to a peak of about 0.4 MPa at 30 seconds because of the He inventory added to the relief header during venting.

Figure 8 shows the 20°K header temperature at the relief valve locations. These temperatures drop rapidly from 20°K to about 7°K.

COMPARISON WITH MEASUREMENTS

In early 1991, the first measurements of quench of a string of two SSC magnets became available. These measurements were performed at the Fermilab String Test Facility,[10] and they provided pressure data at the magnet location and temperature data at the relief valve location. In order to test our model, we simulated the quench venting process for the Fermilab String.

The main differences with the ASST simulation are that the Fermilab string consists of two 40 mm aperture dipole magnets instead of five 50 mm aperture dipole magnets, and that the relief header of the Fermilab string is at room temperature instead of at 20°K.

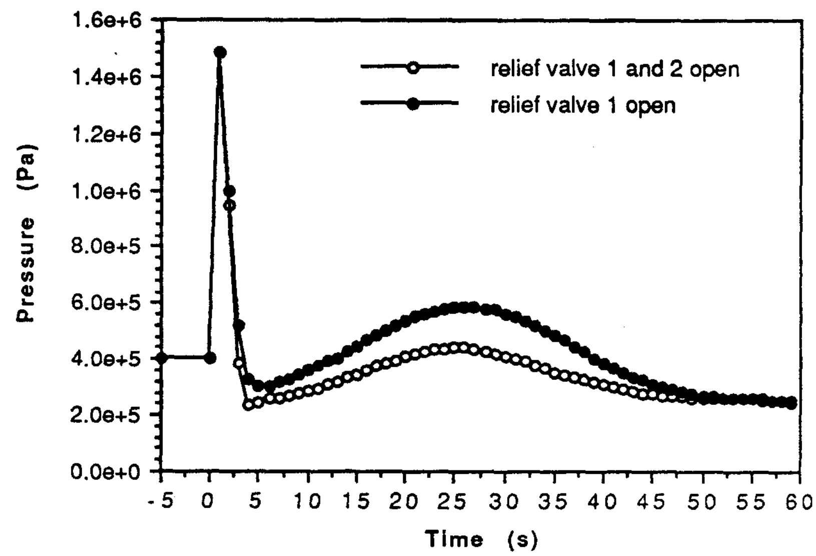

Figure 3. Pressure as a Function of Time for the ASST Quench.

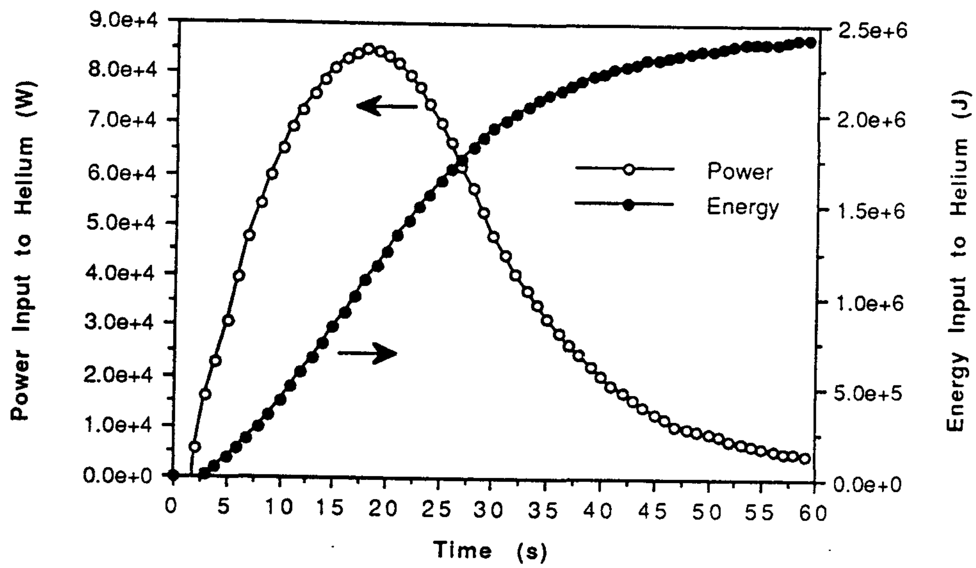

Figure 4. Power and Energy Input to the He as a Function of Time for the ASST Quench.

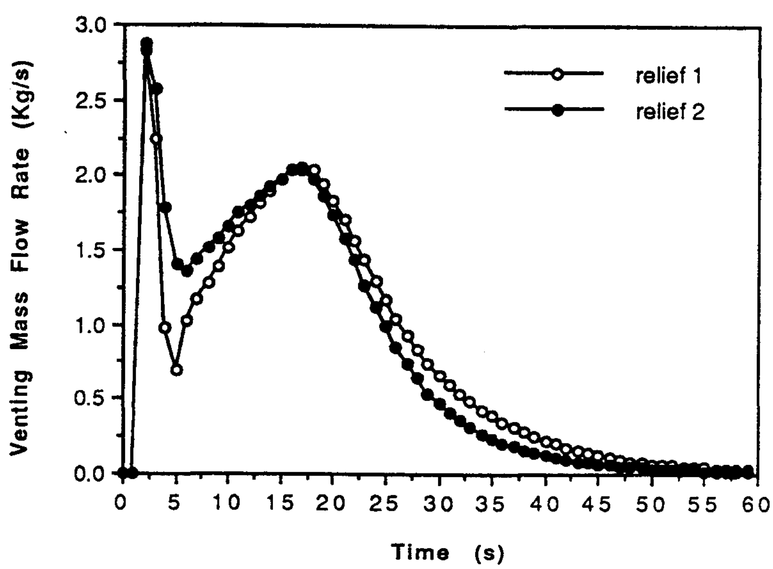

Figure 5. Venting Mass Flow Rate as a Function of Time for the ASST Quench.

Table 2 shows the Fermilab string model boundary conditions, initial conditions, and parameters. Note that we did not attempt to model the room temperature header because the considerable complexity of the problem is beyond the scope of our He model.

Figure 9 shows measured and simulated string pressure as a function of time. The model predicts the correct value for the first peak of 0.85 MPa, showing that the assumption of adiabatic compression for the first stage applies. The agreement between simulation and measurement is excellent during the pressure decay after the second pressure peak, showing that the model predicts the time constant associated with the venting process very well. However, the model does not agree well with the pressure measured during the first and second pressure peaks. Possible reasons for this disagreement are unknown pressure rise in the warm header, vent line cool down effect, and faster venting of the fraction of He inventory located between laminations.

Figure 10 shows measured and simulated temperature as a function of time. Note that the simulation results are for the He temperature in the magnet, and the measurements were done at the relief valve location. We had no temperature measurements for the magnet. The relief was initially at room temperature, and the temperature drops rapidly as liquid He is being vented. It takes more than 5 seconds to approach the level of the liquid He temperature. The simulated venting He temperature when 90% of the He inventory has been vented is about 9°K, and the temperature measured at the relief valve location shows 8°K.

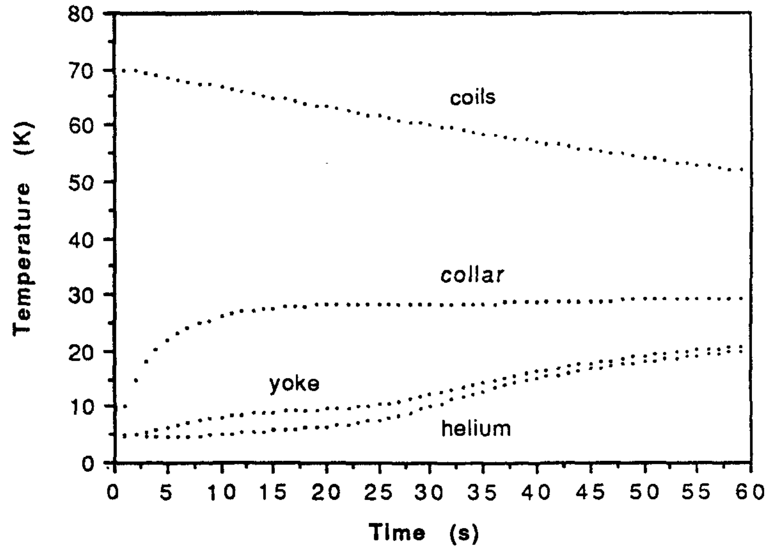

Figure 6. Mid-temperature of the Coils, Collar, Yoke, and He as a Function of Time for the ASST Quench.

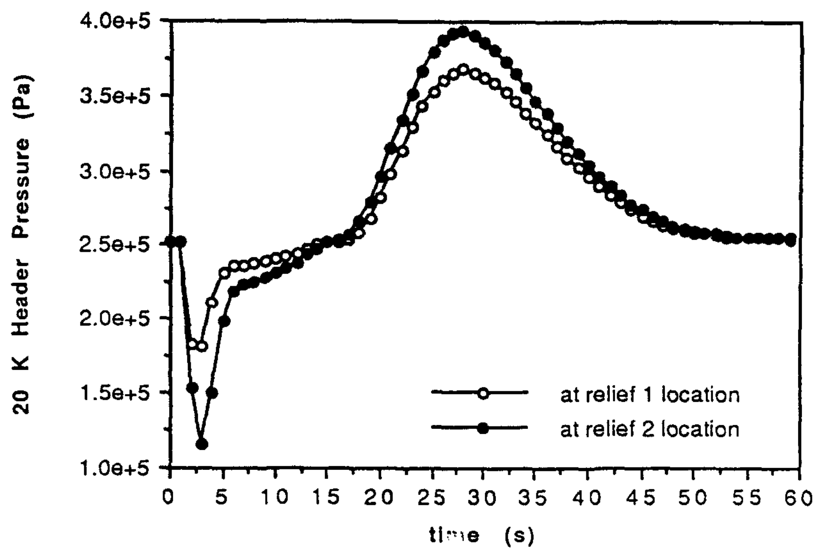

Figure 7. 20K Header Pressure as a Function of Time for the ASST Quench.

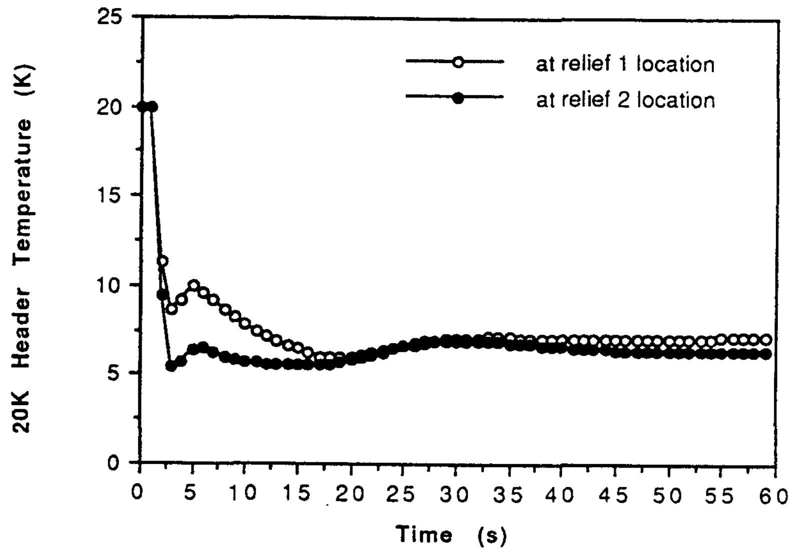

Figure 8. 20K Header Temperature as a Function of Time for the ASST Quench.

Table 2. Boundary Conditions, Initial Conditions, and Parameters for the Fermilab String Test Quench Model.

<u>BOUNDARY CONDITIONS</u>	<u>PARAMETERS</u>
Feed T = 4.5 K	Coil Inner Radius = 0.02 m
Feed P = 0.5 MPa	Coil Outer Radius = 0.04 m
Dewar T = 4.5 K	Kapton Thickness between coil and collar = 6.0×10^{-4} m (24 mil)
Dewar P = 0.12 MPa	Collar Outer Radius = 0.0554 m
Relief Header T = 300 K	Yoke Outer Radius = 0.133 m
Relief Header P = 0.27 MPa	Coolant Channel Diameter = 0.03175 m
<u>INITIAL CONDITIONS</u>	He Volume = 0.3 m^3
Coil T = 70 K	He Mass in coils and in annular passage = 0.8 Kg/dipole
Collar, Yoke, and He T = 4.5 K	Relief Valve Conductance = 0.00068 m^2
String P = 0.5 MPa	
String Flow = 0.05 Kg/s	

In general, the model results agree well with measurements for the parameters of interest; that is, pressure levels, temperature, and timing associated with the venting process are predicted very well. More work is needed in order to understand the disagreement of the pressure change between the first and the second pressure peaks. If this behavior is primarily due to effects such as the pressure rise in the warm header and vent line cooldown during venting, then we expect better agreement for the ASST, where the relief header is at 20°K.

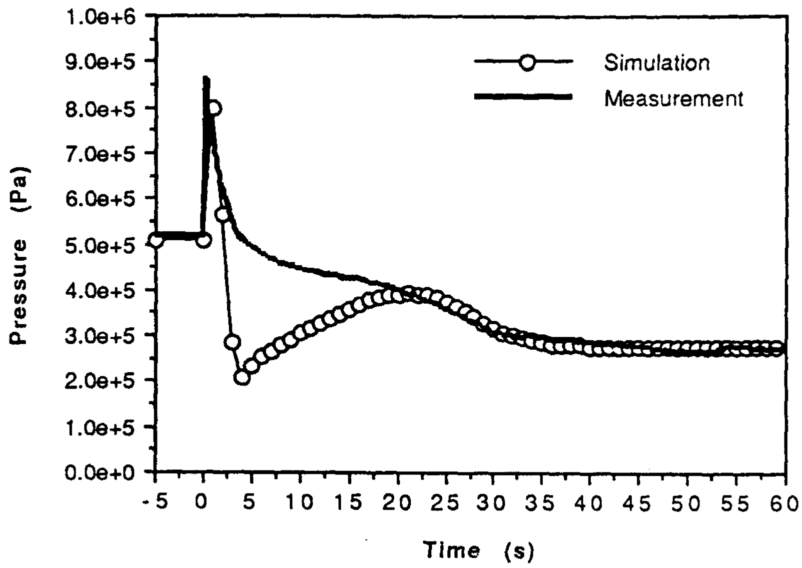

Figure 9. Measured and Simulated String Pressure as a Function of Time for the Fermilab String Test Quench.

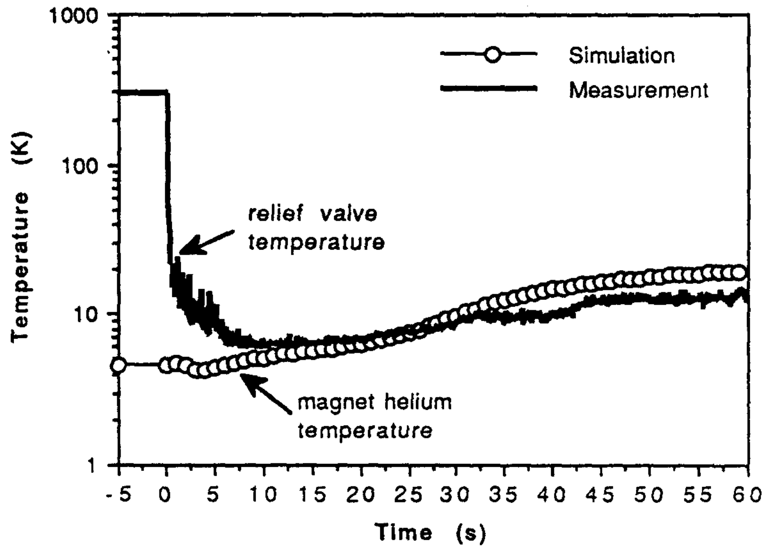

Figure 10. Measured and Simulated Temperature as a Function of Time for the Fermilab String Quench.

CONCLUSIONS

The He venting model presented in this paper was developed primarily to predict the pressure level, temperature level, venting rate, and venting process time constant after an SSC half-cell quench. This is determined in large part by the rate of diffusion of heat from the coils into the bulk of the He that is in the main coolant channels in the iron yoke.

According to our model typically 90% of the initial He inventory is vented in about 30 seconds. A typical peak venting rate is about 2 Kg/s at 17 seconds, and a typical peak power into the He is about 20 KW per dipole magnet at 17 seconds. At 30 seconds, the He temperature is about 9°K. Apart from the initial pressure spike after He expulsion from the coils and in the annular passage, typical pressure levels are between 0.4 and 0.6 MPa for the relief system considered. The cold mass reaches an equilibrium temperature of about 29°K at approximately 200 seconds.

Comparisons of the model results with Fermilab string test measurements show good agreement for the parameters of interest.

NOMENCLATURE

A = heat transfer area, m^2

C = conductance, m^2

C1 = contact conductance between coil and collar, W/m^2-K

C23 = contact conductance between collar and yoke, W/m^2-K

C_p = constant pressure specific heat, J/kg-K

f = Fanning friction factor

G = mass flow rate per unit area, kg/(m^2-s)

H = specific enthalpy, J/kg

h = heat transfer coefficient, W/m^2-K

i = node number in cold mass

k = thermal conductivity, W/m-K

M = sum of all streams entering and exiting a He node

N = number of inlet streams to a He node

P = absolute pressure, Pa

Pr = Prandtl number

Q = heat transfer between the He and the cold mass, W

Re = Reynolds number

r = radial coordinate, m

T = absolute temperature, K

t = time, s

U = specific internal energy, J/kg

V = volume, m^3

W = flow rate, kg/s

z = axial coordinate, m

ρ = density, kg/m^3

θ = angular coordinate, rad

Δr = distance between nodes in cold mass, m

Δp = pressure difference between upstream and downstream He node, Pa

Subscripts

I = inlet stream counter

i = inlet stream, cold mass node number

J = outlet stream counter

1,2,3: coils, collar, and yoke, respectively

REFERENCES

1. Conceptual Design of the Superconducting Super Collider, SSC-SR-2020, March 1986.
2. Site-Specific Conceptual Design of the Superconducting Super Collider, SSCL-SR-1056, July 1990.
3. D. G. Hartzog et al., "Dynamic Modeling and Simulation of the Superconducting Super Collider Cryogenic Helium System," Supercollider 1, Proceedings of the IISSC, New Orleans, 1989.
4. M. A. Hilal et al, "Helium Pressure Rise of Superconducting Super Collider Dipole Magnets Following a Quench," Adv. Cryo. Engr., Vol. **33**, Plenum Press, New York (1988).
5. T.J. Fagan and P.W. Eckels, "Process Control Oriented Quench Analysis of a SSC Magnet," Super Collider 2, Proceedings of the IISSC, Miami Beach, 1990.
6. W. M. Kays, Convective Heat and Mass Transfer, McGraw-Hill, 1966.
7. K. Timmerhaus and T. Flynn, Cryogenic Process Engineering, Plenum Press, New York, 1989.
8. C.F. Colebrook and C.M. White, J. Inst. Civil Eng., Vol. **10**, No. 1, pp.99-118, (1937-1938).
9. R.D. McCarty, "Thermodynamic Properties of Helium-4 from 2 to 1500 K at Pressures to 10^8 Pa," J. Phys. Chem. Ref. Data, **2(41)**, 923-958 (1973).
10. J.C. Theilacker, "Cryogenic Testing at the SSC String Test Facility," Adv. Cryo. Engr., Vol. **33**, Plenum Press, New York, 1988.